brief communication

Osmotic and pharmacological effects of formamide on capacity current, gating current, and sodium current in crayfish giant axons

D. A. Alicata, M. D. Rayner, and J. G. Starkus
Department of Physiology, John A. Burns School of Medicine, and the Bekesy Laboratory of Neurobiology, University of Hawaii, Honolulu, Hawaii 96822

ABSTRACT Internal perfusion with solutions made hyperosmolar by 10% formamide selectively reduces the initial fast component of ON gating current (fast Ig) in crayfish axons. This result parallels the effects of formamide perfusion seen in *Myxicola* giant axons (Schauf, C. L., and M. A. Chuman. 1986. Neural Membranes. Alan R. Liss, Inc., New York. 3–23). However, our findings do not confirm their conclusion that internal formamide has a specific pharmacological effect on fast Ig. Formamide-induced suppression of fast Ig is always associated with changes in linear capacity current, indicating a reduction in the rate of rise of the voltage clamp. Furthermore, this suppression of fast Ig can be reversed when clamp rise time is returned to its control rate by increasing compensation for series resistance (R_s) during formamide perfusion. Increases in R_s during 10% formamide perfusion of up to 5 $\Omega \cdot cm^2$ were measured by evaluating the increase in R_s compensation required to return the following parameters to their control levels: (*a*) peak capacity current, (*b*) peak gating current, (*c*) the voltage maximum of the I_{Na}-V curve, and (*d*) "tau h."

We conclude that hyperosmolar internal formamide increases R_s, reduces clamp speed, and thus selectively suppresses fast Ig. On the other hand, the reversible block of sodium ionic current by internal formamide, reported by Schauf and Chuman, is not eliminated by correcting for series resistance changes during formamide perfusion.

INTRODUCTION

Schauf and Chuman (1986) have reported that internal perfusion with formamide solutions is an effective pharmacological tool for selective removal of the fast component of sodium channel ON gating current (fast Ig) in *Myxicola* giant axons. This selective pharmacological action of formamide has been quoted by Keynes (1986) as evidence suggesting the fractionation of gating charge into two components generated by different regions of the sodium channel molecule.

Both 10 and 20% formamide (45 D) solutions are markedly hyperosmolar. Although this small molecule may be quite membrane-permeable, in giant axon preparations where both internal and external perfusion are used, steep osmotic gradients may be maintained across the axolemma and Schwann cell layer. The effects of hyperosmolar external perfusates (and hypoosmolar internal perfusates) on sodium gating current waveforms have been studied by Stimers et al. (1987) in squid giant axons. They found that the slow "rising phase" of gating current (see Bezanilla and Taylor, 1978; also Armstrong and Gilly, 1979) was removed by outwardly directed water movements. They suggested that the space between the axon and its surrounding Schwann cells (the F-H space, first noted by Frankenhaeuser and Hodgkin, 1956) normally has a high longitudinal resistance (R_{FH}) as compared to that component of the total series resistance (R_s) which derives from the Schwann cell clefts. The additional contribution to total series resistance, produced by this high R_{FH}, should slow clamp rise time in membrane areas not directly beneath Schwann cell clefts. As a result, they concluded, an apparent "rising phase" would be generated from the slowed rise time of the clamp in these relatively undercompensated membrane regions. During outward water movements, when the "rising phase" of gating current disappears, they presumed that the F-H space volume increases. Thus R_{FH} would fall and clamp speed would increase in the previously undercompensated membrane regions. Consistent with that hypothesis, Stimers et al. (1987) noted that outward water movements increased the rate of washout of K^+ from the F-H space and eliminated a small component of linear capacity current with a time course similar to that of the Ig "rising phase."

Stimers et al. (1987) did not study the effects of internal hyperosmolar perfusates. However, Adelman et al. (1977) have reported that changes in F-H space volume appear linearly related to inward or outward water movements, for small osmolar differences. We therefore considered the possibility that inward water movements, generated by the hyperosmolar formamide

Address correspondence to D. A. Alicata, University of Hawaii, Pacific Biomedical Research Center, Bekesy Laboratory of Neurobiology, 1993 East West Road, Honolulu, HI 96822.
Dr. Alicata's electronic mail address is INTERNET: bigtuna! dan @ uhccux.uhcc.hawaii.edu
BITNET: dan % bigtuna @ uhccux.

0006-3495/89/02/347/07 $2.00

perfusate, might increase R_S with or without selective increase in R_{FH}. Such changes should slow clamp rise time, reduce the peak of the linear capacity currents, and might well affect the waveform of ON gating current.

Our data show both a slowing of clamp rise time and reduction in fast Ig after internal perfusion with hyperosmolar formamide solutions. However, fast Ig returns to normal in the presence of formamide when clamp speed is also returned to its control rate by increasing series resistance compensation during formamide perfusion. A preliminary report of this work has been already been presented (Alicata et al., 1988).

METHODS

Medial giant axons from the crayfish, *Procambarus clarkii*, with diameters between 200 and 300 μm, were internally perfused and voltage-clamped using methods previously described (Shrager, 1974; Starkus and Shrager, 1978; Starkus et al., 1984). Temperature was measured with a thermilinear thermistor (Yellow Springs Instrument Co., Yellow Springs, OH) and was controlled to 6.0 ± 0.1°C by Peltier devices (Cambion Corp., Cambridge, MA). Experiments were carried out under computer control using a programmable pulse generator with 12-bit resolution, accurate to within ± 0.1 mV (Adtech Inc., Honolulu, HI). Data traces were also digitized with 12-bit resolution using a Nicolet digital oscilloscope (model 1090A; Nicolet Instrument Corp., Madison, WI) and signal averaged on a Nicolet 1170. Sample intervals of 1 or 2 μs/pt were used in this study. The signal averaged records (4,090 data points) were then transferred and archived onto a hard disk unit (Century Data Systems, Anaheim, CA) via a Dual 83/80 supermicrocomputer (Dual Inc., Berkeley, CA) running the UNIX system V operating system in a multiuser and multitasking mode. To compensate for the lack of real time processing ability on the UNIX system, a master program written in C language controlled the external D/A and A/D devices during data acquisition. This master program also controlled data storage and retrieval, and provided data analysis procedures (including scaling, linear offsets, numerical integration, nonlinear least-squares fitting, and digital filtering).

The linear components of capacity and leakage currents were subtracted directly on the Nicolet 1170 signal averager, using a +P/n procedure (Armstrong and Bezanilla, 1974). A 50-ms conditioning period was interposed at the subtraction holding potential before each P/n pulse. The P/n records were obtained first in each sequence and were saved separately to the disk before test pulse subtraction. These capacity current records were then used for clamp rise time analysis (see below). Exact subtraction of linear capacity currents is routinely obtainable in our axons (see Fig. 1 of Heggeness and Starkus, 1986) provided that sufficient time is allowed for stabilization of R_s after introduction of formamide perfusate.

Estimation of clamp rise time from integrated capacity currents

As shown in Fig. 1, integration of linear capacity current can provide a useful indicator of changes in clamp rise time. However, a slow component of linear capacity current has been reported in crayfish axons (Heggeness and Starkus, 1986), which complicates this technique. In the present data slow capacitance could be resolved into two principal kinetic components using a standard Levenberg-Marquardt fitting algorithm. Typical time constants of these slow components were 180 μs and 1.6 ms, respectively, thus even the faster rate is around 10-fold slower than the falling phase of the fast capacity transient.

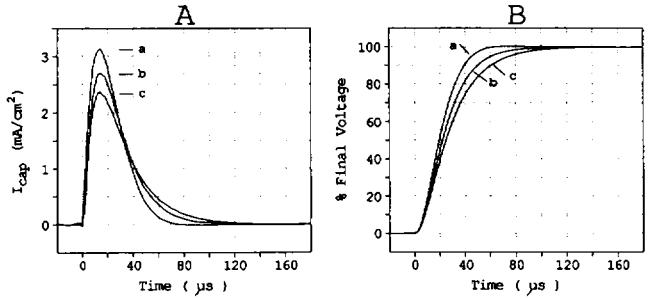

FIGURE 1 Changes in capacity current and clamp rise time produced by changing fractional compensation for series resistance in an equivalent circuit "axon model." In this model series resistance was set equivalent to 10 Ω · cm^2 (±1%) while capacitance was equivalent to 1 μF/cm^2 (±10%). (*A*) Changes in capacity current associated with change in series resistance compensation. Compensation was 100% in trace *a*, 50% in trace *b*, and 0% in trace *c*. Ordinate is "mA/cm^2" for comparison with data traces in later figures. Voltage step from −100 to 0 mV. (*B*) Integration of capacity currents from *A* exemplifies the changes in clamp rise time seen after changes in series resistance compensation. Ordinate is labeled as "% of final voltage," presuming a linear charge–voltage relationship. The total charge moved indicates a capacitance equivalent to 0.93 μF/cm^2, which is consistent with the rated accuracy of the circuit element. Data from model run 880128.

Considering that these slow capacities most probably represent dielectric losses due to nonspecific molecular rearrangements within the membrane's structural proteins and phospholipids, it seems unlikely that they will limit the rate of change of transmembrane voltage under voltage clamp conditions (Almers, 1978). We have therefore stripped out both the 180-μs and 1.6-ms components from integrated records of these capacity currents. Integration of the remaining fast capacity current suggests a membrane capacitance (calculated as $C = Q/V$) of between 0.9 and 1.2 μF/cm^2 in these axons. Clamp rise time was typically 30 μs (to 95% of final voltage) when compensating for 10 Ω cm^2 under control conditions.

Clamp speed and series resistance compensation

Our voltage clamp, like that described by Goldman and Chandler (1986), permits phase-shift adjustment within the series resistance compensation circuit. Thus both fractional compensation for series resistance (see Fig. 1) and the phase-shift setting (see Goldman and Chandler, 1986) can potentially affect clamp rise time. Using an equivalent circuit "axon model" (Fig. 1, *A* and *B*), we show that it is possible to achieve 100% compensation, without instability in the clamp, when phase shift has been carefully adjusted. In internally perfused crayfish axons we find that routine compensation for 10 Ω · cm^2 removes detectable dependence of I_{NA} kinetics on sodium current magnitude (see Fig. 5 *B* and also Starkus et al., 1984). Since the maximum accuracy of this method is ~±1 Ω · cm^2, for peak I_{NA} of 2 mA/cm^2 at 0 mV test potential, series resistance presumably ranges between ~9 and 11 Ω cm^2 in our axons. Series resistance has previously been measured as 6 to 7 Ω · cm^2 in crayfish axons by Shrager and Lo (1982), also using a kinetic method. The phase-shift setting was then fine-tuned until the ratio of peak Ig to Ig at 100 μs was between 2.7 and 3.0 during the initial control period. No readjustments of phase shift were made after subsequent changes in experimental conditions.

Solutions

The external solution used in this study contained: 2.6 mM Mg, 13.5 mM Ca, 210 mM tetramethylammonium (TMA), 243 mM Cl, and 2.3 mM Hepes; adjusted to pH 7.55 and 440 mOsm/liter. Tetrodotoxin (TTX), obtained from Calbiochem-Behring Corp. (La Jolla, CA), was included at 200 nM/liter for all gating current recordings. The control internal solution contained: 230 mM TMA, 60 mM F, 170 mM Glu, and 1 mM Hepes; adjusted to pH 7.35 and 440 mOsm/liter. Formamide perfusate was made up immediately before use by adding 10 ml Formamide (Sigma Chemical Co., St. Louis, MO) to 90 ml of stock internal perfusate; pH was rechecked and total osmolarity was measured to be ~2,900 mOsm/liter. For experiments involving sodium ionic currents, 58 mM Na was added to the external solution by substitution for TMA. The internal perfusate contained 20 mM Na and 210 mM Cs in substitution for the TMA listed above.

Corrections were made for an electrode junction potential of 8–10 mV and this junction potential changed by <1 mV after addition of formamide to the internal perfusate. Electrode drift did not exceed 2–3 mV during the experiments reported here.

RESULTS

As a first step in evaluation of the hypothesis that internal perfusion with hyperosmolar formamide solutions affects gating current by altering the rise time of the voltage clamp, we demonstrate (see Fig. 2 *A*) that changes in series resistance compensation can have substantial impact on the early time course of gating current. Note that these records are shown against a fast time base; the slower components of the waveform are unaffected and consistent with our previous data (Starkus et al., 1981; Heggeness and Starkus, 1986). Trace *a* shows the control record obtained with 10 Ω · cm² R_s compensation (~90–95% of estimated R_s in this axon). Traces *b–f* show the gating currents obtained when compensation for series resistance was readjusted to 9, 8, 7, 5, and 0 Ω · cm², respectively. These records demonstrate progressive reduction in the initial fast component of gating current, as series resistance compensation is reduced. Neither total gating charge nor the time constants of the slower Ig components were affected by change in series resistance compensation.

While recording the gating currents shown in Fig. 2 *A*, we separately recorded the P/n control capacity currents associated with each level of series resistance compensation. These capacity currents are shown in Fig. 2 *B*, traces *a–f*. Peak capacity current falls as the uncompensated component of series resistance increases, indicating a reduction in the maximum rate of rise of clamp voltage, while the falling phase slows significantly. After subtracting the slow components of these control capacity currents (see Methods), the remaining fast linear capacity currents were integrated (see Fig. 2 *C*) to provide a more readily comprehensible measure of clamp rise time. In contrast to the linear relationship between change in R_s compensation and change in peak capacity current shown in Fig. 1 *A*, Fig. 2 *B* demonstrates that change in peak capacity current is here a nonlinear function of the fractional compensation for series resistance. However, the form of this relationship remains similar to that noted by Stimers et al. (1987): the greater the uncompensated fraction of series resistance, the slower the rise time of the clamp (Fig. 2 *C*). The nonlinear response to change in applied series resistance seen here was caused by overcompensation in traces *a* and *b* in each panel. The true

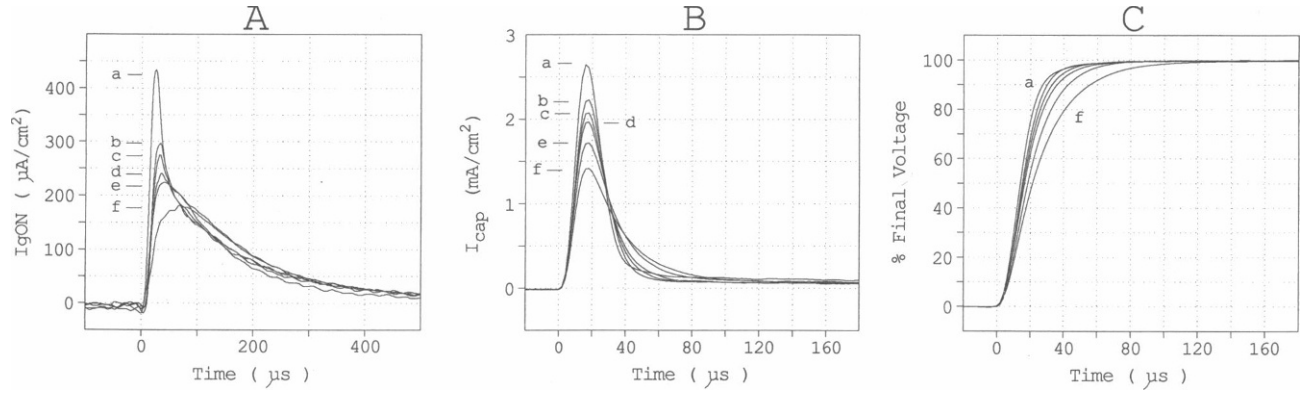

FIGURE 2 Changes in series resistance compensation affect gating current, capacity current, and clamp rise time. (*A*) Gating currents from the same axon recorded using different levels of R_s compensation. Trace *a*, 10; *b*, 9; *c*, 8; *d*, 7; *e*, 5; *f*, 0 Ω · cm². Total gating charge integrated over a 2-ms period was, in trace *a*, 43; *b*, 43; *c*, 44; *d*, 44; *e*, 44; and *f*, 44 nC/cm². Holding potential, −120 mV; test potential, 0 mV. (*B*) Capacity currents for a 40 mV P/3 control voltage step, recorded at the same R_s compensation levels as in *A*. Voltage step from −180 to −140 mV; traces labeled as above. The slow capacity current component appears as a plateau at times >60–80 µs. (*C*) Integrated fast capacity transients indicate rate of rise of clamp voltage. Slow components were subtracted (see Methods) after integration of the traces from *B*. Traces were then normalized to facilitate comparison of rates. Errors in maximum charge did not exceed ±5% before normalization. Only traces *a* and *f* are labeled here; intervening traces appear in alphabetical order. Membrane capacitance was calculated as 1.1 µF/cm² in this axon. All data are from axon 871217.

series resistance in this axon was apparently closer to 8 $\Omega \cdot cm^2$ than to the routinely applied 10 $\Omega \cdot cm^2$ used throughout this study (see Methods).

Since changes in R_s compensation also affect clamp rise time in the axon "model" (see Methods), a cause and effect relationship can be presumed between the clamp rise time changes (indicated in Fig. 2 *C*) and the changes in gating current waveform shown in Fig. 2 *A*. For the traces obtained with 10 $\Omega \cdot cm^2$ series resistance compensation (trace *a* in each figure), the peak of the gating current occurs well before final voltage is reached and a clear "fast Ig" component is visible. In contrast, when series resistance compensation is turned off (trace *f* in each figure), the gating current peaks considerably later, closer to the time at which final potential is reached, and fast Ig cannot be separately identified. These kinetic shifts did not involve any change in total gating charge, which remained at 43 nC/cm^2 in Fig. 2 *A* for trace *a* and 44 nC/cm^2 for trace *f*. We conclude that slowing the clamp does not "remove" fast Ig. Fast Ig only becomes readily apparent in gating current records when the rate of rise of the clamp approaches the eigenvalue characteristic of this very rapid component.

Accurate measurement of the fast Ig kinetic is not possible in the data presented here, since the clamp has not yet settled at this stage of the gating current waveform. However significant change in peak Ig occurs for quite small changes in clamp rate. Thus between records *a* and *c* of Fig. 2 *A* there is a 36% suppression of peak Ig while the time to peak increases from 20 to 26 μs. For comparison the clamp time constant, determined from the equivalent traces in Fig. 2 *C* increased from 7.5 to 10.5 μs.

Having clarified the relationships between R_s compensation, clamp rise time, and gating current waveform in control axons, we now demonstrate the effects of internal formamide perfusion on gating current (see Fig. 3 *A*) and capacity current (Fig. 3 *B*) in crayfish axons. In view of the low normal osmolarity of crayfish body fluids (~400 mosM), by comparison with those of *Myxicola,* we have used 10% formamide solution as the standard in our work rather than the 20% formamide solution used by Schauf and Chuman (1986). The sevenfold increase in internal osmolarity produced by 10% formamide in our axons is approximately equivalent to the increase in osmolarity produced by 20% formamide in *Myxicola* axons. However, water flux should be proportional to the difference in osmotic activity between internal and external solutions. Thus the outward water flux produced by 10% formamide in crayfish axons may be only about half that generated by 20% formamide in Schauf and Chuman's study. Nevertheless the 10% formamide perfusate produces a pronounced, reversible, suppression of both the fast component of Ig (see Fig. 3 *A*) and the P/n capacity currents (see Fig. 3 *B*), such that a 33% reduction occurs in peak gating current. After integration of the capacity current and removal of the slow components (see Methods), Fig. 3 *C* demonstrates a 25% slowing of clamp rate during formamide perfusion. No corrections were made here for possible changes in series resistance, which remained compensated at 10 $\Omega \cdot cm^2$ in both control and formamide records. Qualitative comparison between Figs. 2 *A* and 3 *A* suggests that formamide perfusion may have increased series resistance, thus slowing the clamp by leaving the axon effectively undercompensated.

Quantitative comparison between Figs. 2 *A* and 3 *A* is not appropriate since, as noted above, the linearity of the response to change in series resistance may be markedly

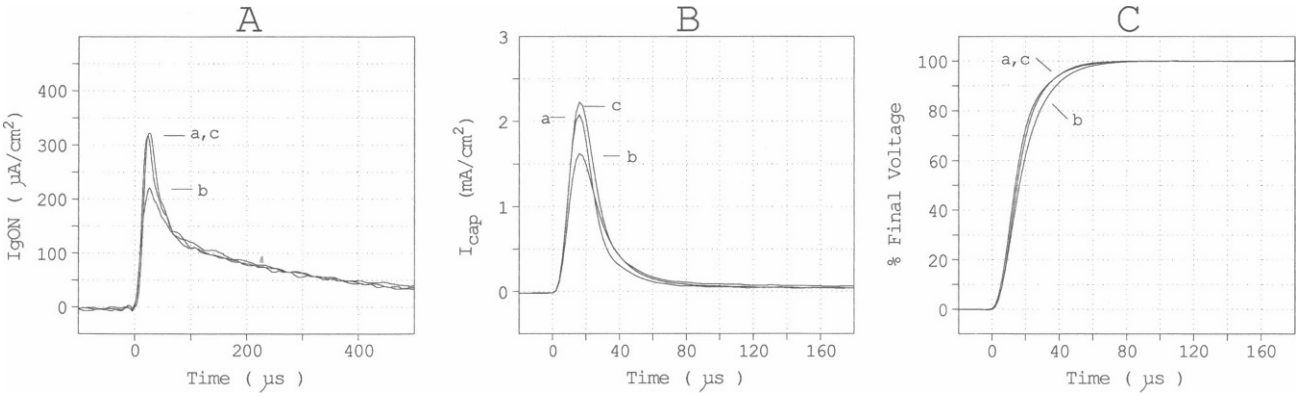

FIGURE 3 Reversible suppression of fast Ig and capacity current during internal perfusion with 10% formamide. (*A*) Gating currents at −20 mV before (trace *a*), during (trace *b*), and after (trace *c*) internal formamide perfusion. The first 500 μs of each data trace is shown here to permit clear visualization of the changes in fast Ig. Integration of these gating current traces over a 2-ms period gives the following total gating charge movements: trace *a*, 34; *b*, 34; *c*, 33 nC/cm^2. Holding potential, −120 mV. (*B*) Control P/3 capacity currents corresponding to the gating current records of *A*. Voltage step from −180 to −146.7 mV. (*C*) Clamp rise times for gating current traces of *A*, as indicated by integration of the fast components of capacity currents in *B*. Membrane capacitance was 1.2 $\mu F/cm^2$ in this axon. All data are from axon 871115.

affected by failure to achieve exact R_s compensation under control conditions. We have therefore used a "null" method to quantify the formamide-induced change in effective R_s. In this method R_s compensation was progressively increased during formamide perfusion, until control peak height of both capacity current and gating current was regained (see Fig. 4). The change in applied R_s compensation should then indicate the formamide-induced change in R_s.

In Fig. 4, where this "null" method is demonstrated, peak capacity current was returned to control magnitude by increasing R_s compensation from 10 to 15 $\Omega \cdot cm^2$ in 10% formamide (see Fig. 4 *B*, trace *c*). Some instability in the clamp appears in the trace, which could have been removed by fine tuning of the phase-shift circuit (see Methods). We made no such adjustments here, however, since phase-shift adjustment also affects clamp rate. Nevertheless our data suggest that formamide perfusion increased R_s by as much as 5 $\Omega \cdot cm^2$ in this axon.

The gating current records for this same experiment are shown in Fig. 4 *A*. The apparent reduction in fast Ig is clearly visible in the formamide record (trace *b*) obtained before readjustment of series resistance compensation. However fast Ig returns to control magnitude (see trace *c*) in the record obtained with series resistance compensation increased to 15 $\Omega \cdot cm^2$. Thus, after correcting for formamide-induced changes in clamp speed, there seems no evidence for direct, selective, pharmacological effects of formamide on fast Ig (at concentrations readily achievable in crayfish giant axons).

Suppression of sodium ionic conductance by internal formamide (see Schauf and Chuman, 1986) is also readily observed in crayfish giant axons. Fig. 5 *A* shows the maximum inward current regions of two *I-V* curves obtained during and after internal perfusion with 10% formamide, from a holding potential of −120 mV. Series resistance compensation was 10 $\Omega \cdot cm^2$ for both curves. It may be noted that the peak inward current occurs at ~−15 mV in formamide and ~−10 mV in control conditions. Such a shift in peak voltage could have resulted either from increase in R_s in the presence of hyperosmolar internal formamide, or from a formamide-induced voltage-sensitive pharmacological block of sodium channels, or from a combination of both effects. Fig. 5 *B* shows the results of a preliminary study on the mechanisms of formamide-induced sodium current suppression. The three curves identified by open symbols show *I-V* curves obtained in the absence of formamide at different holding potentials (−120, −100, and −90 mV). Despite an almost threefold change in current magnitude the peak voltage is not significantly affected, indicating the effectiveness of our series resistance compensation under control conditions. In this plot the formamide data (*solid symbols*) has been corrected for the expected 5 $\Omega \cdot cm^2$ error in series resistance indicated by our Fig. 4 data. For inward I_{Na} of 1 mA/cm^2 and a series resistance increase of 5 $\Omega \cdot cm^2$, the required correction is a 5 mV shift to the right along the voltage axis. This correction shifts the peak voltage into line with the three control curves. Formamide-induced suppression of sodium current seems somewhat greater at the more depolarized potentials shown, suggesting that formamide may block sodium channels by a voltage-sensitive process. Fig. 5*C* shows control inward sodium current at −10 mV (trace *a*) and the reduced sodium current seen at −15 mV during formamide perfusion (trace *b*). The kinetic simi-

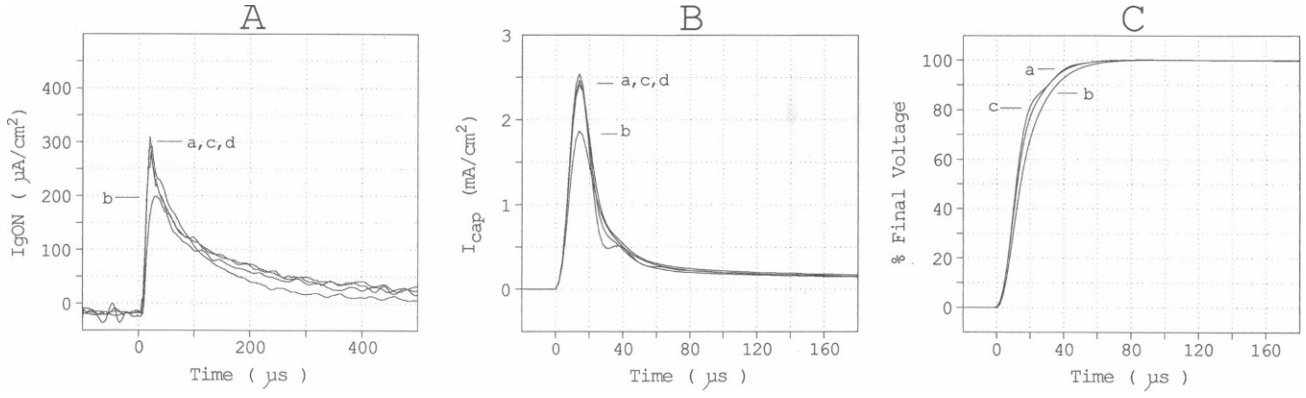

FIGURE 4 Both fast Ig and capacity current return to normal when R_s is increased from 10 to 15 $\Omega \cdot cm^2$ during internal formamide perfusion. (*A*) Gating currents before (trace *a*), during (traces *b* and *c*), and after (trace *d*) perfusion with 10% formamide. R_s compensation was set to 10 $\Omega \cdot cm^2$ in traces *a*, *b*, and *d*, but was increased to 15 $\Omega \cdot cm^2$ in trace *c*. Holding potential was −120 mV; step to 0 mV test potential. (*B*) P/3 capacity currents corresponding to the gating current records in *A*. Voltage step from −180 to −140 mV. Note the incipient instability visible in record *c*. (*C*) Clamp rise times obtained by integration of the fast capacity components from *B* (traces *a*, *b*, and *c*). Membrane capacitance was calculated as 0.9 $\mu F/cm^2$ in this axon. All data from axon 880425.

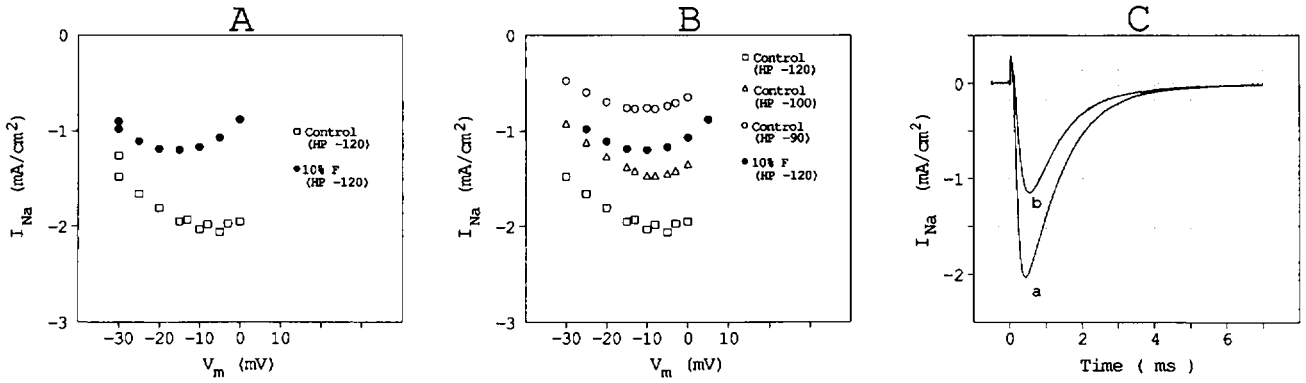

FIGURE 5 Block of inward sodium current during internal perfusion with 10% formamide. (*A*) Peak inward current before (*open squares*) and during (*solid circles*) formamide perfusion. Peak inward current is reduced by formamide and the maximum occurs at −15 mV, as compared with ~ −10 mV in the control curve. (*B*) Control peak inward currents (*open symbols*) obtained from three different holding potentials: −120 mV (*squares*); −100 mV (*triangles*), and −90 mV (*circles*). The potential at which maximum peak current occurs remains ~ −10 mV for each curve. Also shown (*solid circles*) are formamide points from *A* shifted to the right by 5 mV (to correct for an assumed R_s error of 5 Ω · cm^2 when peak current is close to 1 mA/cm^2. (*C*) Comparison of control sodium current at −10 mV (trace *a*) with sodium current at −15 mV in presence of internal formamide (trace *b*). Tau h was 1.05 ms in trace *a* and 1.02 ms in trace *b*. All data from axon 880125, recorded using 10 Ω · cm^2 series resistance compensation.

larity of these records is demonstrated by "tau h" measurements: tau h was 1.05 ms for trace *a*, 1.02 ms for trace *b*, and 1.3 ms for the control record at −15 mV test potential (not shown). Thus I_{NA} falling phase kinetics also confirm a 5 Ω · cm^2 increase in R_s during formamide perfusion.

DISCUSSION

A small component of Ig with faster kinetics than the major charge-carrying component was first reported in crayfish axons by Starkus et al. (1981). This fast component appeared related to the sodium channel control mechanism since both fast Ig and the slower gating current components were equally reduced by depolarized holding potentials, and to the same extent as sodium ionic current. However, fast Ig appears insensitive to fast inactivation (Starkus and Rayner, 1987). Keynes (1986) similarly notes a fast, inactivation-insensitive, component in his gating current records. On the other hand, Schauf and Chuman (1986) reported that formamide selectively affects a "fast Ig," which was also suppressed by fast inactivation. If formamide affects the inactivation-sensitive component of gating current by a selective pharmacological mechanism, then we would not have expected a suppression of the fast Ig in our preparation. On the other hand, if formamide acts on gating current as an osmotic agent, then it may simply suppress whichever component is closest in kinetics to the rate of rise of the clamp under control conditions.

Here we confirm the observation of Schauf and Chuman (1986) that formamide selectively reduces fast Ig (see Fig. 3), although we note that capacity current is also reduced while clamp rise time slows during internal formamide perfusion. However, formamide-induced slowing of clamp rise time can be reversed when series resistance compensation is increased (see Fig. 4), as if R_s rises during perfusion with hyperosmolar formamide solution. Thus no evidence remains for the selective pharmacological action of formamide on fast Ig proposed by Schauf and Chuman (1986), once clamp rise time has been returned to its control value.

The data presented here are not sufficient to provide definitive characterization of the mechanism by which internal formamide perfusion reduces I_{NA}. Formamide block appears to be tonic and no more than marginally voltage sensitive (see Fig. 5), thus resembling the block produced by internal tetramethylammonium ions in these same axons (see Fig. 3 of Starkus and Heggeness, 1986).

Finally, although hyperosmolar formamide perfusate increases R_s, our data do not demonstrate the induced "rising phase" in Ig, which would have been expected from the squid axon data provided by Stimers et al. (1987) and Adelman et al. (1977). In squid axons inward water movement reduces the volume of the F-H space, predicting a relatively greater increase for the uncompensatable R_{FH} component than for the compensatable components of total R_s. There are two lines of evidence which suggest that such expectations may not be applicable to crayfish axons.

(*a*) Gating currents in crayfish axons do not typically show any "rising phase" which outlasts the major component of capacity current (see Fig. 2 *A* and Starkus et al., 1981; Swenson, 1983; Heggeness and Starkus, 1986). Even in the presence of formamide, we find no indication

of any "rising phase" once R_s compensation has been adjusted so as to return peak capacity current to its control height (see Fig. 4, trace *c*). In crayfish axons, therefore, R_{FH} may remain small relative to total R_s, even in the presence of markedly hyperosmolar internal perfusates. However, the control clamp rise time in the present study was about threefold slower than that used by Stimers et al. (1987), although the kinetics of gating current are two- to threefold faster in crayfish than in squid (Starkus et al., 1981). Thus clamp speed in this study may not have been fast enough for resolution of R_{FH}-induced rising phases.

(*b*) The nature of the periaxonal space in crayfish axons has been investigated by Shrager et al. (1983) using a combination of voltage clamp, thin section, and freeze fracture techniques. The rate of washout of K^+ ions from the periaxonal space was found to be 25-fold faster in crayfish than in squid axons, while there was no signficant difference between the washout rates for sodium and potassium ions. At the ultrastructural level, a complex lattice of tubules was found to cross the innermost glial layers in crayfish axons. No such structure has been reported for squid, where a narrow periaxonal space opens into clefts between the Schwann cells at intervals of 5–13 μm. By contrast, in crayfish, the spacing between openings of the tubular lattice was only ~0.2 μm. Shrager et al. (1983) concluded that crayfish sodium channels are located in regions with relatively unrestricted access to bulk extracellular fluid. Thus effective R_{FH} may well remain small, by comparison with total R_s, in crayfish axons under most experimental conditions.

We thank Dr. Peter Ruben for his helpful comments and Richard Foulk for his programming assistance.

This work was supported by the National Institutes of Health through both research grant NS21151-04 (to J. G. Starkus) and RCMI award 3G12 RR03061-02. Additional support was received from the American Heart Association (Hawaii Affiliate), the University of Hawaii Research Council, and BRSG 2S07 RR07026 awarded by the Biomedical Research Support Grant Program, Division of Research Resources, National Institutes of Health.

Received for publication 10 June 1988 and in final form 14 September 1988.

REFERENCES

Adelman W. J., J. Moses, and R. V. Rice. 1977. An anatomical basis for the resistance in series with the excitable membrane of the squid axon. *J. Neurocytol.* 6:621–646.

Alicata, D. A., M. D. Rayner, and J. G. Starkus. 1988. Osmotic effect of formamide on sodium channel gating currents in crayfish giant axon. *Biophys. J.* 53:538a. (Abstr.)

Almers, W. 1978. Gating currents and charge movements in excitable membranes. *Rev. Physiol. Biochem. Pharmacol.* 82:96–190.

Armstrong, C. M., and F. Bezanilla. 1974. Charge movement associated with the opening and closing of the activation gates of the Na channels. *J. Gen. Physiol.* 63:533–552.

Armstrong, C. M., and W. F. Gilly. 1979. Fast and slow steps in the activation of sodium channels. *J. Gen. Physiol.* 74:691–711.

Bezanilla, F., and R. E. Taylor. 1978. Temperature effects on gating currents in the squid giant axon. *Biophys. J.* 23:479–484.

Frankenhaeuser, B., and A. L. Hodgkin. 1956. The after-effects of impulses in the giant nerve fibers of *Loligo*. *J. Physiol.* (*Lond.*). 131:341–376.

Goldman, L., and R. E. Chandler. 1986. Geographical distribution and inactivation kinetics in internally perfused *Myxicola* giant axons. *Biophys. J.* 49:761–766.

Heggeness, S. T., and J. G. Starkus. 1986. Saxitoxin and tetrodotoxin. Electrostatic effects on sodium channel gating current in crayfish giant axons. *Biophys. J.* 49:629–643.

Keynes, R. D. 1986. Properties of the sodium gating current in the squid giant axon. *Ann. NY Acad. Sci.* 479:431–438.

Schauf, C. L., and M. A. Chuman. 1986. Mechanisms of sodium channel gating revealed by solvent substitution. *In* Neural Membranes. Alan R. Liss, Inc., New York. 3–23.

Shrager, P. 1974. Ionic conductance changes in voltage clamped crayfish axons at low pH. *J. Gen. Physiol.* 64:666–690.

Shrager, P., and M-V. C. Lo. 1982. Influence of ionic current on Na^+ channel gating in crayfish giant axon. *Nature* (*Lond.*). 296:450–452.

Shrager, P., J. G. Starkus, M-V. C. Lo, and C. Peracchia. 1983. The periaxonal space of crayfish giant axons. *J. Gen. Physiol.* 82:221–244.

Starkus, J. G., and M. D. Rayner. 1987. Immobilizable and non-immobilizable components of gating charge in crayfish giant axon. *Biophys. J.* 51:434a. (Abstr.)

Starkus, J. G., and P. Shrager. 1978. Modification of slow sodium inactivation in nerve after internal perfusion with trypsin. *Am. J. Physiol.* 4:C238–244.

Starkus, J. G., B. D. Fellmeth, and M. D. Rayner. 1981. Gating currents in the intact crayfish giant axon. *Biophys. J.* 35:521–533.

Starkus, J. G., S. T. Heggeness, and M. D. Rayner. 1984. Kinetic analysis of sodium channel block by internal methylene blue in pronased crayfish giant axons. *Biophys. J.* 46:205–218.

Stimers, J. R., F. Bezanilla, and R. E. Taylor. 1987. Sodium channel gating currents. Origin of the rising phase. *J. Gen. Physiol.* 89:521–540.

Swenson, R. P. 1983. A slow component of gating current in crayfish giant axons resembles inactivation charge movement. *Biophys. J.* 41:245–249.